Supplementary Information (SI) for Journal of Materials Chemistry C.

Efficient solar steam generation enabled by nanolamellar λ-Ti_3O_5 based on designing the bandgap through morphology modulation

Tingting Yuan [a], Yudong Wang [a], Na Jin [a], Jinwen Ye [a,b] *

[a]*School of Materials Science & Engineering, Sichuan University, Chengdu, 610065, China*

[b]*Sichuan Vanadium&Titanium Industrial Technology Institute, Sichuan University, Chengdu, 610065, China*

*Corresponding author.

E-mail: yjw550@163.com

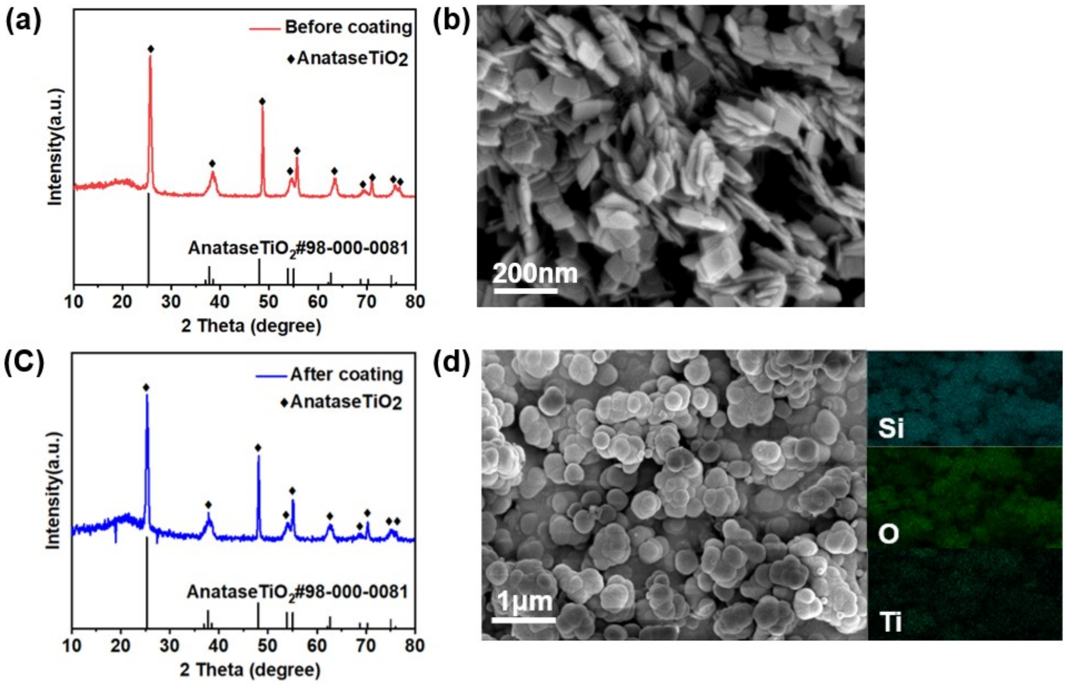

Fig. S1. (a) XRD patterns of anatase TiO_2; (b) SEM image of TiO_2 before coating SiO_2; (c) XRD patterns of core-shell TiO_2@SiO_2; (d) SEM imagine and EDS plane-scanning elemental mappings of core-shell TiO_2@SiO_2.

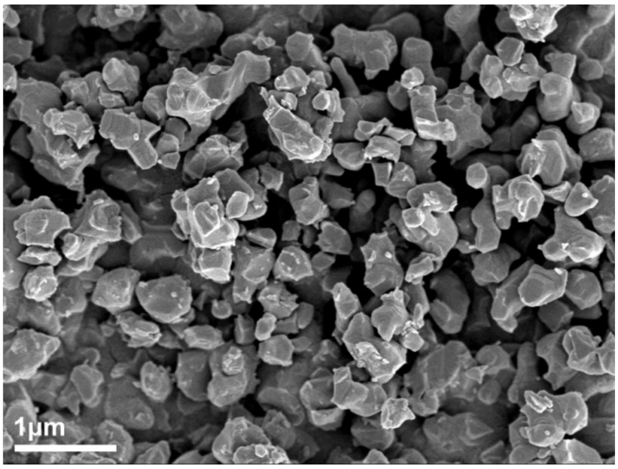

Fig. S2. SEM image of λ-Ti_3O_5 without coating of SiO_2

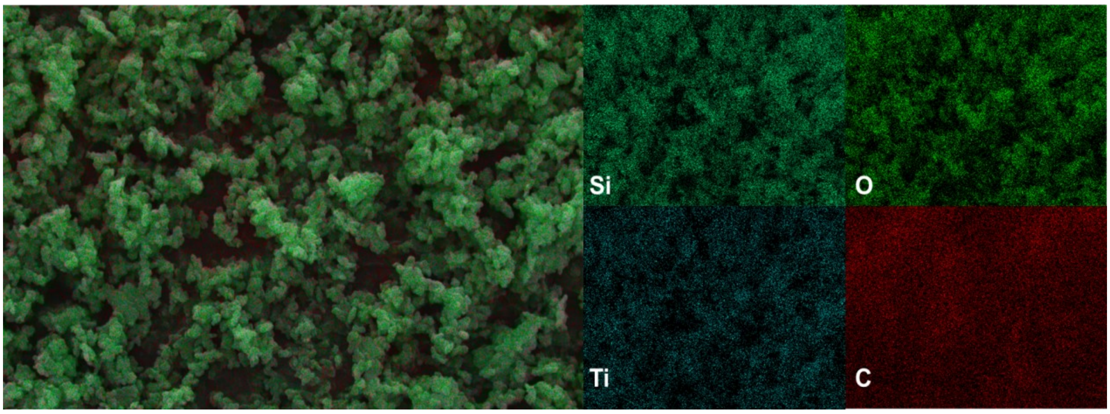

Fig. S3. EDS image of core-shell $Ti_3O_5@SiO_2$

Eq. S1.

The solar absorptance is calculated from the ratio of the total solar radiation absorbed by the material to the incident radiation: [1,3]

$$\eta_{solar} = \frac{\int_{200}^{2500} E(\lambda)[1 - R(\lambda)]d\lambda}{\int_{200}^{2500} E(\lambda)d\lambda} \tag{S1}$$

where $E(\lambda), R(\lambda)$ are the AM1.5G spectrum from the sun, the reflectance of sunlight at different wavelengths by Ti_nO_{2n-1}.

Eq. S2-S8.

The heat absorbed by the sample during the illumination period, which we calculate using [2]:

$$Q_{absorbed} = C_s m_s (T_s - T_{env}) \tag{S2}$$

where C_s, m_s, T_s and T_{env} indicate the specific heat capacity, the mass and the average temperature of the pill, and the temperature of the environment, respectively.

The heat lost by convection, radiation and conduction is calculated by the following equation [2,3]:

$$Q_{convection} = hA_s(T_s - T_{env})t \tag{S3}$$

$$Q_{radiation} = \varepsilon_s A_s \sigma (T_s^4 - T_{env}^4)t \tag{S4}$$

$$Q_{conduction} = \lambda_{PE} A_s \frac{dT}{dx} t \quad \text{(S5)}$$

where A_s, T_s, ε_s indicate the surface area (including both the circular area and the lateral area), the surface temperature, the emissivity of the pill, σ is the Stefan-Boltzmann constant, h is the convection coefficient, and λ_{PE} and $\frac{dT}{dx}$ are the thermal conductivity and the temperature gradient of the PE foam, respectively.

The total heat loss can be obtained by summing the above three components,

$$Q_{loss} = Q_{convection} + Q_{radiation} + Q_{conduction} \quad \text{(S6)}$$

Hence, the photothermal conversion efficiency can be calculated as follows [2,4]

$$\eta = \frac{Q_{loss} + Q_{absorbed}}{Q_{solar} \eta_{solar}} \quad \text{(S7)}$$

$$Q_{solar} = C_{opt} P A_s^{top} t \quad \text{(S8)}$$

where C_{opt}, P, and A_s^{top} are the solar concentration, the standard solar irradiation power, and the area directly above the pill used to absorb sunlight, respectively.

Eq. S9-S17.

To further quantify the enhancement effect of each titanium oxide material on the evaporation rate, the evaporation rate u in Fig. 5c was calculated from the following equation [5]:

$$u = \frac{\Delta m}{At} \quad \text{(S9)}$$

where u, Δm, A, and t represent the rate of evaporation, the change in mass of fresh water in the evaporation system in a certain time, the area used for evaporation, and the evaporation time.

The enthalpy of evaporation and the solar to steam efficiency can be calculated by using the following thermodynamic equation. The heat absorbed by the surface of the 2D evaporator during t time of solar irradiation is [2]

$$Q_{absorbed} = Q_{solar} - Q_{reflection} \quad \text{(S10)}$$

$$Q_{solar} = C_{opt}PA_{2D}t \quad \text{(S11)}$$

$$Q_{reflection} = (1 - \eta_{solar})Q_{solar} \quad \text{(S12)}$$

where A_{2D} is the effective area of 2D evaporator absorbing sunlight.

Similarly, the energy absorbed by the 2D evaporator is partially used to evaporate fresh water, but is also lost through by convection, radiation and conduction. Considering all these, the energy used for evaporation of clear water is [3]

$$Q_{vaporization} = Q_{absorbed} - Q_{convervtion} - Q_{radiation} - Q_{conduction} \quad \text{(S13)}$$

the convection heat loss is defined by Newton's law of cooling [6,7]

$$Q_{convection} = hA_{2D}(T_{2D} - T_{env})t \quad \text{(S14)}$$

and the radiation heat loss is calculated by the Stefan–Boltzmann equation[8]

$$Q_{radiation} = \varepsilon_{2D}A_{2D}\sigma(T_{2D}^{4} - T_{env}^{4})t \quad \text{(S15)}$$

and the remaining energy lost by conduction is [8]

$$Q_{conduction} = C_{bulk\ water}m_{bulk\ water}\Delta T_{bulk\ water} \quad \text{(S16)}$$

where $C_{bulk\ water}$, $m_{bulk\ water}$ and $\Delta T_{bulk\ water}$ are indicate the specific heat capacity, the mass and the temperature rise of the bulk water, respectively.

Meanwhile, the energy consumed to evaporate fresh water can be calculated from [8]

$$Q_{vaporization} = \dot{m}\Delta H_{vap} + \dot{m}C_{bulk\ water}(T_{2D} - T_{bulk\ water}) \quad \text{(S17)}$$

where $\dot{m}$ and ΔH_{vap} are the net evaporated mass of water under solar insolation and the phase change enthalpy of bulk water.

Hence, the enthalpy of evaporation of clear water can be obtained by calculating $Q_{vaporization}$ and substituting it into the above equation.

Table. S1. Parameters used to calculate photothermal conversion efficiency

C_{opt}	1	A_s	1.72787×10^{-4} m^2
C_s^{Ti4O7}	0.723 J g^{-1} K^{-1}	m_s	0.4 g
$C_s^{\lambda-Ti3O5}$	0.770 J g^{-1} K^{-1}	T_s^{Ti4O7}	330.45 K
$C_s^{\beta-Ti3O5}$	0.682 J g^{-1} K^{-1}	T_{env}	298.15 K
h	5 W m^{-2} K^{-1}	$T_s^{\lambda-Ti3O5}$	332.65 K
σ	5.68×10^{-8} W m^{-2} K^{-4}	$T_s^{\beta-Ti3O5}$	318.95 K
ε_s	0.97	T_s^{NL-T3}	334.45 K
η_{solar}	0.922	ΔT	27.3 K
C_s^{NL-T3}	0.776 J g^{-1} °C^{-1}	λ_{PE}	0.029 W m^{-2} k $^{-1}$

Table. S2. Parameters used to calculate solar-to-steam efficiency and enthalpy of water evaporation

C_{opt}	1	A_{2D}	1.5205×10^{-3} m^{-2}
P	1 kW m^{-2}	$m_{bulk\ water}$	0.05 kg
t	1 h	T_{2D}	310.85 K
ε_{2D}	0.97	T_{env}	298.15 K
h	5 W m^{-2} K^{-1}	$\Delta T_{bulk\ water}$	2.4 K
σ	5.68×10^{-8} W m^{-2} K^{-4}	$T_{bulk\ water}$	303.25 K

$C_{bulk\ water}$	4.2×10^3 J kg^{-1} K^{-1}	$u_{1\ sun}$	1.79 kg m^{-2} h^{-1}
η_{solar}	0.8865	u_{dark}	0.22 kg m^{-2} h^{-1}

Table. S3. Comprehensive performance of other 3D evaporation systems

PTCMs	Absorption [%]	Evaporation rate [kg m^{-2} h^{-1}]	Efficiency [%]	Ref.
nanocarbon composite of graphene oxide and carbon nanotubes	-	1.59	100	[9]
mixed metal oxide	-	2.04	nearly 100	[10]
polypyrrole	99.2	1.70	93.8	[11]
λ-Ti_3O_5	96.4	6.09	95.92	[12]
carbonized bamboo	99.2	3.13	132	[13]
nanoink-stained PVA sponge	96.5	2.15	-	[14]
bamboo leaf-derived carbon and macroporous melamine foam	94	2.29	93.95	[15]
nature SP, PDA, PSBMA, cellulose nanofibers and melanin hybrids	97	3.79	97.7	[16]
cellulose and alginate	97	1.33	90.6	[17]
hydrophobic pyrrole	95	3.65	-	[18]
flower–like graphene	-	3.0	93.83	[19]
porous carbon polyhedron	99	2.74	98.2	[20]
MnO_2	85	2.67	89.5%	[21]

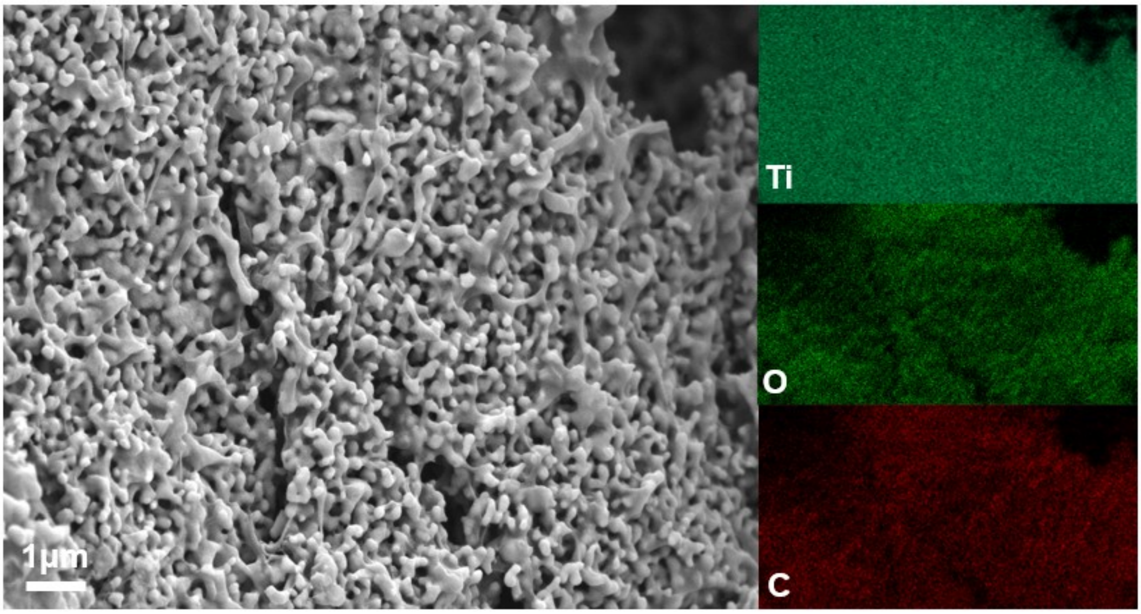

Fig. S4. SEM imagine and EDS plane-scanning elemental mappings of 3D evaporation system

References

[1] M. Gao, L. Zhu, C. K. Peh, G. W. Ho, Solar absorber material and system designs for photothermal water vaporization towards clean water and energy production, *Energy Environ. Sci.,* 2019, **12**, 841-864.

[2] X. Liu, D. D. Mishra, X. Wang, H. Peng, C. Hu, Towards highly efficient solar-driven interfacial evaporation for desalination, *J. Mater. Chem. A,* 2020, **8**, 17907-17937.

[3] F. Cao, K. McEnaney, G. Chen, Z. Ren, A review of cermet-based spectrally selective solar absorbers, *Energy Environ. Sci.,* 2014, **7**, 1615-1627.

[4] G. Ni, G. Li, Svetlana V. Boriskina, H. Li, W. Yang, T. Zhang, G. Chen, Steam generation under one sun enabled by a floating structure with thermal concentration, *Nat. Energy,* 2016, **1**,

16126.

[5] R. Zhu, D. Wang, J. Xie, Y. Liu, M. Liu, S. Fu, Salt-resistant Schiff base cross-linked superelastic photothermal cellulose aerogels for long-term seawater desalination, *Chem. Eng. J.,* 2022, **427**, 131618.

[6] P. Zhang, Q. Liao, H. Yao, H. Cheng, Y. Huang, C. Yang, L. Jiang, L. Qu, Three-dimensional water evaporation on a macroporous vertically aligned graphene pillar array under one sun, *J. Mater. Chem. A,* 2018, **6**, 15303-15309.

[7] X. Li, W. Xu, M. Tang, L. Zhou, B. Zhu, S. Zhu, J. Zhu, Graphene oxide-based efficient and scalable solar desalination under one sun with a confined 2D water path, *Proc. Nat. Acad. Sci.,* 2016, **113**, 13953-13958.

[8] K. Yin, S. Yang, J. Wu, Y. Li, D. Chu, J. He, J.-A. Duan, Femtosecond laser induced robust Ti foam based evaporator for efficient solar desalination, *J. Mater. Chem. A,* 2019, **7**, 8361-8367.

[9] S. Hong, Y. Shi, R. Li, C. Zhang, Y. Jin, P. Wang, Nature-Inspired, 3D Origami Solar Steam Generator toward Near Full Utilization of Solar Energy, *ACS Appl. Mater. Interfaces,* 2018, **10**, 28517-28524.

[10] Y. Shi, R. Li, Y. Jin, S. Zhuo, L. Shi, J. Chang, S. Hong, K.-C. Ng, P. Wang, A 3D Photothermal Structure toward Improved Energy Efficiency in Solar Steam Generation, *Joule,* 2018, **2**, 1171-1186.

[11] Y. Wang, C. Wang, X. Song, M. Huang, S. K. Megarajan, S. F. Shaukat, H. Jiang, Improved light-harvesting and thermal management for efficient solar-driven water evaporation using 3D photothermal cones, *J. Mater. Chem. A,* 2018, **6**, 9874-9881.

[12] B. Yang, Z. Zhang, P. Liu, X. Fu, J. Wang, Y. Cao, R. Tang, X. Du, W. Chen, S. Li, H. Yan, Z. Li, X. Zhao, G. Qin, X.-Q. Chen, L. Zuo, Flatband λ-Ti3O5 towards extraordinary solar steam generation, *Nature,* 2023, **622**, 499-506.

[13] Y. Bian, Q. Du, K. Tang, Y. Shen, L. Hao, D. Zhou, X. Wang, Z. Xu, H. Zhang, L. Zhao, S. Zhu, J. Ye, H. Lu, Y. Yang, R. Zhang, Y. Zheng, S. Gu, Carbonized Bamboos as Excellent 3D Solar Vapor-Generation Devices, Adv. Mater. Technol., 2018, **4**, 1800593.

[14] Z. Deng, L. Miao, P.-F. Liu, J. Zhou, P. Wang, Y. Gu, X. Wang, H. Cai, L. Sun, S. Tanemura, Extremely high water-production created by a nanoink-stained PVA evaporator with embossment structure, *Nano Energy,* 2019, **55**, 368-376.

[15] J. Jiang, R. Yang, F. Zeng, S. Tu, Biomass-derived three-dimensional robust solar evaporator for efficient steam generation, water purification and salt-resistant desalination, *Chem. Eng. J.,* 2024, **481**, 148289.

[16] W. Ma, W. Cao, M. Cui, H. Lu, R. Xiong, C. Huang, Biomass-derived 3D evaporator with antifouling and salt-rejecting toward solar-enabled steam generation, desalination, and electricity generation, *Chem. Eng. J.,* 2023, **478**, 147404.

[17] J. Yuan, X. Lei, C. Yi, H. Jiang, F. Liu, G. J. Cheng, 3D-printed hierarchical porous cellulose/alginate/carbon black hydrogel for high-efficiency solar steam generation, *Chem. Eng. J.,* 2022, **430**, 132765.

[18] C. Wei, X. Zhang, S. Ma, C. Zhang, Y. Li, D. Chen, H. Jiang, Z. Xu, X. Huang, Ultra-robust vertically aligned three-dimensional (3D) Janus hollow fiber membranes for interfacial solar-driven steam generation with salt-resistant and multi-media purification, *Chem. Eng. J.,* 2021, **425**, 130118.

[19] H. Wang, X. Wen, K. Liu, Q. Liu, G. Hu, H. Liu, Y. She, R. Niu, T. Tang, J. Gong, Interfacial solar-driven steam and electricity co-generation using Hydrangea-like graphene by salt-assisted carbonization of waste polylactic acid, *SusMat*., 2024, **4**, e242.

[20] H. Liu, L. Liu, Z. Fan, J. Liu, H. Wang, X. Wen, G. Hu, K. Liu, R. Niu, J. Gong, Transforming waste polyester into porous carbon polyhedron for interfacial solar steam and hydrovoltaic electricity co-generation, *Chem. Eng. J.,* 2024, **85**, 149690.

[21] R. Niu, J. Ren, J.J. Koh, L. Chen, J. Gong, J. Qu, X. Xu, J. Azadmanjiri, J. Min, Bio-inspired sandwich-structured all-day-round solar evaporator for synergistic clean water and electricity generation, *Adv. Energy Mater.*, 2023, **13**, 2302451.